Iterative Group Detection and Decoding for Large MIMO Systems

Jun Won Choi, Byungju Lee, and Byonghyo Shim

Abstract: **Recently, a variety of reduced complexity soft-in soft-output detection algorithms have been introduced for iterative detection and decoding (IDD) systems. However, it is still challenging to implement soft-in soft-output detectors for MIMO systems due to heavy burden in computational complexity. In this paper, we propose a soft detection algorithm for MIMO systems which performs close to the full dimensional joint detection, yet offers significant complexity reduction over the existing detectors. The proposed algorithm, referred to as *soft-input soft-output successive group (SSG) detector*, detects a subset of symbols (called a *symbol group*) successively using a deliberately designed preprocessing to suppress the inter-group interference. In fact, the proposed preprocessor mitigates the effect of the interfering symbol groups successively using *a priori* information of the undetected groups and *a posteriori* information of the detected groups. Simulation results on realistic MIMO systems demonstrate that the proposed SSG detector achieves considerable complexity reduction over the conventional approaches with negligible performance loss.**

Index Terms: **Codebook-based precoding, group detection, iterative detection and decoding, LTE-Advanced, multiple-input multiple-output (MIMO).**

I. INTRODUCTION

OVER the years, multiple-input multiple-output (MIMO) systems having a large number of transmit and receive antennas are of great interest as a means to achieve high spectral efficiencies and reliability in future wireless systems. In order to achieve high rates on rich scattering environments, a cost-effective receiver performing the MIMO detection and the channel decoding is required. As a practical scheme achieving this goal, the *iterative detection and decoding* (IDD) technique has been popularly used [1], [2]. In the IDD systems, both the MIMO detector and the channel decoder exploit the soft-output obtained from each other as prior information. As a soft-input soft-output channel decoder, max-log-map decoder [3] is widely used, and as a MIMO detector, *a posteriori probability* (APP) bit detector [1] is well-known. By performing the MIMO detection and channel decoding in an iterative fashion, IDD achieves the performance close to the optimal joint detectors. One drawback of the APP bit detector is that its complexity grows exponentially with the dimension of the systems and modulation order. To address the complexity issue, a number of low-complexity soft-input soft-output detection algorithms have been proposed. *Tree search algorithms* [4], originally designed for maximum likelihood detection (MLD) [5], [6], were extended to perform soft detection for IDD systems. This approach includes the *list sphere decoding* (LSD) [1], [7], [8], fixed complexity sphere decoding (FCSD) [9], and chase detector [10]. Besides, various reduced complexity detection algorithms including the K-best algorithm [6], [11], and the list sequential stack search (LSSS) [12] have been proposed. While these approaches exhibit fairly decent complexity for moderate system sizes (e.g., 4×4 MIMO in LTE standard), the complexity is still a major issue for MIMO systems with large transmit/receive antennas. In order to cope with high dimensionality of the system, group detection strategies, partitioning the symbol vector to be detected into multiple subgroups, have been studied [13]–[17].

In this paper, we introduce a low-complexity soft-input soft-output MIMO detector for the IDD systems. The proposed MIMO detection technique, referred to as a soft-output successive group (SSG) detector, builds on a group detection strategy [13], [14], [18]–[21]. Although reduction in the dimension will be beneficial in computational complexity, due to the interference of other subgroups (i.e., inter-group interference), receiver suffers from the performance degradation. There have been some approaches mitigating the inter-group interference via linear preprocessing [15], [18]–[20]. These include linear transformation with the decision feedback interference cancellation [15], subspace projection-based decorrelator [18], [19], and maximal ratio combining [20]. Although these approaches are effective in reducing the complexity of the uncoded systems, they are not suitable for IDD systems since they do not consider the soft symbol information from the channel decoder.

The proposed SSG detection algorithm exploits the soft information of the other symbol groups to improve the detection quality of the target symbol group. Toward this end, SSG detector partitions the symbol vector into the multiple subgroups and then processes each symbol group successively. Starting from the subgroup with the best signal-to-interference-plus-noise ratio (SINR), group detection is performed sequentially, generating *a posteriori* log-likelihood ratio (LLR) of the target symbol group. Operations for each group consists of 1) the inter-group interference cancellation followed by the linear preprocessing to suppress the residual interference and 2) the detection of the target group to generate the *a posteriori* LLRs. In the first step (preprocessing step), inter-group interference cancella-

This paper is specially handled by EICs and Divisions Editor with the help of three anonymous reviewers in a fast manner.

This work was supported in part by ICT R&D program of MSIP/IITP, B0126-15-1017, Spectrum Sensing and Future Radio Communication Platforms and the National Research Foundation of Korea (NRF) grant funded by the Korean government (MSIP) (2014R1A5A1011478).

This research was also supported by Basic Science Research Program through the National Research Foundation of Korea (NRF) grant funded by the Ministry of Education (NRF-2014R1A1A2055805).

J. Choi is with Dept. of Electrical Engineering, Hanyang University, Seoul Korea, email: junwchoi@hanyang.ac.kr.

B. Lee and B. Shim are with Institute of New Media and Communications and School of Electrical and Computer Engineering, Seoul National University, Seoul, Korea, email: {bjlee, bshim}@snu.ac.kr.

Digital object identifier 10.1109/JCN.2015.000108

tion and residual interference suppression are performed. Both the *a posteriori* LLRs of the already processed groups (henceforth referred to as causal group) and the *a priori* LLRs of nonprocessed groups (noncausal group) are exploited for the best possible inter-group interference cancellation. Due to the use of *latest soft information* in the inter-group interference cancellation, the successive cancellation is effective and in fact performs better than the parallel cancellation approach based on *a priori* LLRs [17]. To further suppress the residual interference after the interference cancellation, MMSE based linear interference suppression is applied. In essence, the proposed approach is distinct from the existing preprocessing methods in the sense that the linear MMSE preprocessor exploits the *latest soft information* of other groups and thus the effect of intergroup interference suppression improves as the number of iterations increases.

Another important issue to be considered to support high-dimensional MIMO systems is a heavy burden in the feedback link, in particular for frequency division duplexing (FDD) systems. Since the direct feedback of channel state information (CSI) requires substantial amount of resources in the feedback link, codebook-based precoding might be a reasonable option for the FDD-based MIMO systems.[1] Main operation of the receiver employing codebook-based precoding is to choose a precoder maximizing a predefined performance metric (e.g., spectral efficiency). Since the performance metric is usually a function of the SINR, accurate estimation of SINR for each subgroup is crucial in maximizing throughput of the system. Note that unlike the system employing the linear receiver technique, it is very difficult to find the closed form expression of the SINR of the nonlinear detection scheme. In this work, we propose a simple scheme that allows the MIMO systems using the SSG detector to quickly adapt its precoder based on the channel variations. Two main ingredients of our scheme are the parametric SINR estimation and the rate maximizing codebook precoding. By selecting the best possible precoder matching to the estimated SINR of the SSG detector, the link performance can be improved considerably. In fact, we observe from simulations on the realistic MIMO channels that the SSG detector outperforms the existing group detectors while keeping the computational complexity low.

The rest of this paper is organized as follows. In Section II, we review the IDD system and the soft-output detection algorithm. In Section III, we describe the proposed SSG detection algorithm. In Section IV, we discuss the SINR estimation and codebook-based precoding for the SSG detector. In Section V, we provide the simulation results and conclude the paper in Section VI.

We briefly summarize notations used in this paper. Uppercase and lowercase letters written in boldface denote matrices and vectors, respectively. Superscripts $(\cdot)^T$ and $(\cdot)^H$ denote transpose and conjugate transpose (hermitian operator), respectively. $\|\cdot\|^2$ indicates an ℓ_2-norm of a vector. $CN(0,\sigma^2)$ denotes a circularly symmetric complex Gaussian distribution with variance σ^2. $E_x[\cdot]$ denotes expectation over the random variable x. The notations for covariance matrices are given by $\mathrm{Cov}(\mathbf{x},\mathbf{y}) = \mathbf{E}[\mathbf{x}\mathbf{y}^{\mathbf{H}}] - \mathbf{E}[\mathbf{x}]\mathbf{E}[\mathbf{y}]^{\mathbf{H}}$ and $\mathrm{Cov}(\mathbf{x}) = \mathrm{Cov}(\mathbf{x},\mathbf{x})$.

[1] Although time division duplexing (TDD) might be advantageous in reducing the CSI feedback overhead, there are many pros and cons between two (see, e.g., [22]) and still many carriers employ FDD systems.

II. SOFT-INPUT SOFT-OUTPUT DETECTION

In this section, we review the IDD principle and soft-input soft-output detection algorithm.

A. Iterative Detection and Decoding

The relationship between the transmit symbol and the received signal vector in the MIMO systems is expressed as

$$\mathbf{y_n} = \mathbf{H_n}\mathbf{x_n} + \mathbf{n_n} \tag{1}$$

where $\mathbf{x_n} \in \mathbb{C}^{\mathbb{N}\times\mathbb{1}}$ is the signal vector whose entries are the symbols transmitted at time n, $\mathbf{y_n} \in \mathbb{C}^{\mathbb{L}\times\mathbb{1}}$ and $\mathbf{n_n} \in \mathbb{C}^{\mathbb{L}\times\mathbb{1}}$ are the received signal and noise vectors received at time n, and $\mathbf{H_n} \in \mathbb{C}^{\mathbb{L}\times\mathbb{N}}$ is the MIMO channel matrix. In the context of MIMO systems, N and L represent the number of transmit and receive antennas, respectively. For convenience, we will omit time index n if there is no risk of confusion. When the transmitter precoding is applied, one can further express $\mathbf{H} = \mathbf{H}'\mathbf{P}$ where $\mathbf{H}'$ and $\mathbf{P}$ are the $L \times N$ spatial channel matrix and $N \times N$ precoding matrix, respectively. When the information being transmitted is encoded, which is true for most wireless MIMO systems, the receiver can accurately estimate the transmit symbol vectors $\{\mathbf{x_n}\}$ from the received vectors $\{\mathbf{y_n}\}$ via a *maximum a posteriori* (MAP) detection. While the joint detection and decoding via MAP receiver requires tremendous complexity even for moderate system size, the IDD achieves near optimal performance with relatively low cost by performing the symbol detection and channel decoding iteratively. In the transmitter, a rate R_c channel encoder is used to convert a sequence of independent identically distributed (i.i.d.) binary information bits $\{b_i\}$ to an encoded sequence $\{c_i\}$. The bit sequence $\{c_i\}$ is scrambled using a random interleaver $\prod$ and then mapped into a sequence of symbol vectors using a 2^Q-ary quadrature amplitude modulation (QAM) symbol alphabet. We henceforth denote the interleaved bits associated with the kth symbol x_k as $\overline{c}_{k,1},\cdots,\overline{c}_{k,Q}$. Due to the use of the interleaver, the interleaved bits are approximately statistically independent of one another.

The IDD receiver consists of two main blocks; the detector and the channel decoder. The detector generates the extrinsic LLR of $\overline{c}_{k,i}$ using the observation $\mathbf{y}$ and *a priori* information delivered from the channel decoder. Using the standard noise model $\mathbf{n} \sim CN\left(0,\sigma_n^2\mathbf{I}\right)$, one can express the *a posteriori* LLR as [1]

$$\begin{aligned} L_{\mathrm{post}}\left(\overline{c}_{k,i}\right) &= \ln\frac{Pr(\overline{c}_{k,i}=+1|\mathbf{y})}{Pr(\overline{c}_{k,i}=-1|\mathbf{y})} \\ &= \ln\frac{\sum_{\mathbf{x}\in\mathbf{X}_{\mathbf{k,i}}^{+1}}\exp(\psi(\mathbf{x}))}{\sum_{\mathbf{x}\in\mathbf{X}_{\mathbf{k,i}}^{-1}}\exp(\psi(\mathbf{x}))} \end{aligned} \tag{2}$$

where

$$\psi(\mathbf{x}) \triangleq -\tfrac{1}{\sigma_n^2}\|\mathbf{y}-\mathbf{H}\mathbf{x}\|^2 + \textstyle\sum_{l=1}^{N}\sum_{m=1}^{Q}\overline{c}_{l,m}\frac{L_{\mathrm{pri}}(\overline{c}_{l,m})}{2} \tag{3}$$

and $X_{k,i}^{\pm 1}$ is the set of all combinations of $\mathbf{x}$ satisfying $\overline{c}_{k,i} = \pm 1$. $L_{\mathrm{pri}}(\overline{c}_{k,i})$ is the *a priori* LLR defined as $L_{\mathrm{pri}}(\overline{c}_{k,i}) = \ln Pr(\overline{c}_{k,i} = +1) - \ln Pr(\overline{c}_{k,i} = -1)$[2]. Once $L_{\mathrm{post}}(\overline{c}_{k,i})$

[2] We use $\overline{c}_{k,i} \in \{-1,1\}$ instead of $\{0,1\}$ for notational convenience.

is computed, the extrinsic LLR is obtained from $L_{\rm ext}(\overline{c}_{k,i}) = L_{\rm post}(\overline{c}_{k,i}) - L_{\rm pri}(\overline{c}_{k,i})$. These extrinsic LLRs are de-interleaved and then delivered to the channel decoder. The channel decoder computes the extrinsic LLRs for the coded bits $\{c_i\}$ and then feeds them back to the detector. These operations are repeated until a suitably chosen convergence condition is satisfied or the loop number equals a predefined maximal value.

B. Complexity Reduction via Search Space Limitation

Since the direct computation of the *a posteriori* LLR in (2) involves marginalization over 2^{NQ} symbol candidates, the computational complexity of the APP bit detector grows exponentially with the transmit antenna size N. However, by limiting the search space into the set of reliable symbol candidates (denoted as Φ), complexity of the APP bit detector can be reduced. The approximated version of *a posteriori* LLR over this reduced set Φ becomes

$$L_{\rm post}\left(\overline{c}_{k,i}\right) \approx \ln \frac{\sum_{\mathbf{x}\in \mathbf{X}_{\mathbf{k,i}}^{+1} \bigcap \mathbf{\Phi}} \exp\left(\psi\left(\mathbf{x}\right)\right)}{\sum_{\mathbf{x}\in \mathbf{X}_{\mathbf{k,i}}^{-1} \bigcap \mathbf{\Phi}} \exp\left(\psi\left(\mathbf{x}\right)\right)}. \tag{4}$$

One can further reduce the complexity by applying the max-log-MAP approximation, i.e., $\ln(e^x + e^y) \approx \overset{*}{\max}(x,y) \triangleq \max(x,y) + \delta$ [3].[3] In this case, $L_{\rm post}\left(\overline{c}_{k,i}\right)$ in (4) becomes

$$L_{\rm post}\left(\overline{c}_{k,i}\right) \approx \underset{\mathbf{x}\in \mathbf{X}_{\mathbf{k,i}}^{+1} \bigcap \mathbf{\Phi}}{\overset{*}{\max}} \psi\left(\mathbf{x}\right) - \underset{\mathbf{x}\in \mathbf{X}_{\mathbf{k,i}}^{-1} \bigcap \mathbf{\Phi}}{\overset{*}{\max}} \psi\left(\mathbf{x}\right). \tag{5}$$

By controlling the size of Φ, one can alleviate the computational overhead at the expense of marginal performance loss. This, however, is not a desirable solution for MIMO systems since the reduction in the number of candidates will cause a severe performance loss. Allowing large number of candidates is also undesirable since it will simply make the system unimplementable. In the next section, we introduce the group detection technique that achieves near optimal performance yet requires comparable complexity to the linear receiver.

III. SOFT-INPUT SOFT-OUTPUT SUCCESSIVE GROUP (SSG) DETECTION

A block diagram of the SSG detector is depicted in Fig. 1. In a nutshell, the SSG detector partitions the symbol vector into multiple subgroups and then processes each symbol group successively. Group detection consists of two steps: 1) The linear preprocessing step and 2) joint group detection step. As mentioned, the quality of the group detection improves by suppressing the inter-group interference and the linear preprocessor performs this task by exploiting the *a posteriori* LLRs of the causal groups and the *a priori* LLRs of noncausal groups simultaneously. In generating the extrinsic LLRs for each sub group, any soft detection scheme such as APP bit detector and LSD [1] can be used. After processing all symbol groups, the extrinsic LLRs for those groups are delivered to the channel decoder.

[3]For equality to hold, $\delta = \ln(1+e^{-|x-y|})$. Nonlinear mapping from $|x-y|$ to δ can be implemented using a look-up table.

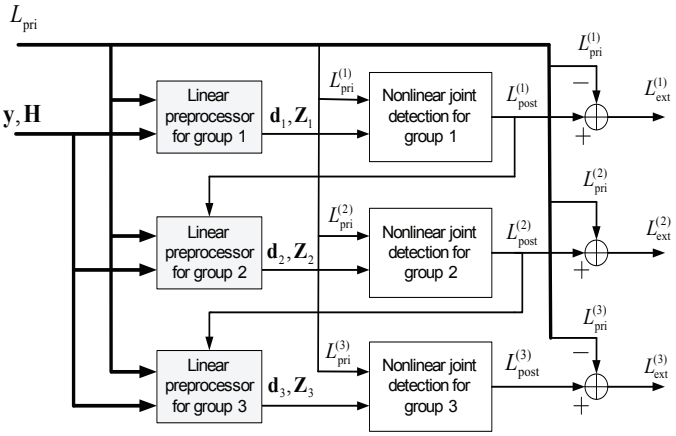

Fig. 1. The block diagram of the SSG detector. As an example, we illustrate the case of three group partitioning. $L_{\rm pri}^{(i)}$, $L_{\rm post}^{(i)}$, and $L_{\rm ext}^{(i)}$ denote the *a priori*, *a posteriori*, extrinsic LLRs of the symbol group i, respectively.

A. Symbol Ordering and Grouping

In the first step of the SSG detection, the symbols are ordered and processed based on post-detection SINR [23], which is beneficial for the remaining groups to be detected and also reduces the chance of error propagation. Suppose the symbol vector $\mathbf{x}$ is partitioned into multiple subgroups $\mathbf{x_1},\cdots,\mathbf{x_J}$, then we have

$$\mathbf{y} = \begin{bmatrix}\mathbf{H_1} & \cdots & \mathbf{H_J}\end{bmatrix} \begin{bmatrix}\mathbf{x_1}\\ \vdots \\ \mathbf{x_J}\end{bmatrix} + \mathbf{n} \tag{6}$$

where $\mathbf{x_i} \in C^{N_i \times 1}$ and $\mathbf{H_i} \in C^{L\times N_i}$ are the vectors representing the ith symbol group and the corresponding sub-matrix of $\mathbf{H}$, respectively, $\mathbf{y} \in C^{L\times 1}$ is the vector whose element is the signal acquired from each of the L receive antennas, and N_i is the number of symbols in the ith symbol group. Without loss of generality, we assume that a small number in the subscript corresponds to the stronger symbols (in terms of post-detection SINR) so that the symbols are processed in the order from $\mathbf{x_1}$ to $\mathbf{x_J}$. In what follows, we focus on the detection of a target group $\mathbf{x_j}$, and hence $\{\mathbf{x_1},\cdots,\mathbf{x_{j-1}}\}$ and $\{\mathbf{x_{j+1}},\cdots,\mathbf{x_J}\}$ become the causal and noncausal groups in view of the target group $\mathbf{x_j}$.

B. Linear MMSE preprocessing

Rewriting (6), we have

$$\mathbf{y} = \mathbf{H_j x_j} + \underbrace{\mathbf{H_{1:j-1}x_{1:j-1}}}_{\text{causal groups}} + \underbrace{\mathbf{H_{j+1:J}x_{j+1:J}}}_{\text{noncausal groups}} + \mathbf{n} \tag{7}$$

where $\mathbf{x_{n:m}}$ and $\mathbf{H_{n:m}}$ $(n<m)$ are $[\mathbf{x_n^H},\mathbf{x_{n+1}^H},\cdots,\mathbf{x_m^H}]^{\mathbf{H}}$ and $[\mathbf{H_n},\cdots,\mathbf{H_m}]$, respectively. In essence, the main purpose of the preprocessing is to suppress the effect of interfering symbol groups via a linear operator. The preprocessing is divided into two steps: 1) Soft inter-group interference cancellation and 2) MMSE estimation of the ideal observed signal without interference.

B.1 Soft Interference Cancellation

In the first step, inter-group interferences of the causal symbol groups (obtained from the *a posteriori* LLRs) and the noncausal

groups (obtained from the *a priori* LLRs) are cancelled from the received signal $\mathbf{y}$. That is,

$$\hat{\mathbf{y}}_j = \mathbf{y} - \mathbf{H_{1:j-1}}\overline{\mathbf{x}}^{\mathrm{post}} - \mathbf{H_{j+1:J}}\overline{\mathbf{x}}^{\mathrm{pri}} \tag{8}$$

where $\overline{\mathbf{x}}^{\mathrm{post}} = [\overline{x}_1^{\mathrm{post}}, \cdots, \overline{x}_{j-1}^{\mathrm{post}}]^T$ is the mean vector of $\mathbf{x_{1:j-1}}$ generated from the *a posteriori* LLRs and $\overline{\mathbf{x}}^{\mathrm{pri}} = [\overline{x}_{j+1}^{\mathrm{pri}}, \cdots, \overline{x}_J^{\mathrm{pri}}]^T$ is the mean vector of $\mathbf{x_{j+1:J}}$ constructed by the *a priori* LLRs, respectively. Note that $\hat{\mathbf{y}}_j$ is obtained by subtracting the soft estimates of causal and non-causal symbol groups from the received vector $\mathbf{y}$. Note that $\overline{x}_j^{\mathrm{post}}$ is given by [1], [24]

$$\overline{x}_i^{\mathrm{post}} = \sum_{\theta\in\Theta} \theta \prod_{k=1}^{Q} \underbrace{\frac{1}{2}\left(1 + \overline{c}_{i,k}\tanh\left(L_{\mathrm{post}}(\overline{c}_{i,k})/2\right)\right)}_{Pr(\overline{c}_{i,k})} \tag{9}$$

where the set Θ includes all possible constellation points. One can obtain the similar expression for $\overline{x}_i^{\mathrm{pri}}$.

B.2 Residual Interference Suppression

Using (7) and (8), the modified received signal after the soft interference cancellation becomes

$$\begin{aligned}\hat{\mathbf{y}}_j =& \mathbf{H_j x_j} + \mathbf{H_{1:j-1}}\left(\mathbf{x_{1:j-1}} - \overline{\mathbf{x}}^{\mathrm{post}}\right) \\ &+ \mathbf{H_{j+1:J}}\left(\mathbf{x_{j+1:J}} - \overline{\mathbf{x}}^{\mathrm{pri}}\right) + \mathbf{n}.\end{aligned} \tag{10}$$

In order to further suppress the residual interference from the modified received signal, we perform the estimation of the ideal received signal $\mathbf{z_j} = (\mathbf{H_j x_j} + \mathbf{n})$. The LMMSE estimate of $\mathbf{z_j}$ based on the observation $\hat{\mathbf{y}}_j$ is

$$\hat{\mathbf{z}}_j = \mathrm{Cov}(\mathbf{H_j x_j} + \mathbf{n}, \hat{\mathbf{y}}_j)\mathrm{Cov}(\hat{\mathbf{y}}_j)^{-1}\hat{\mathbf{y}}_j \tag{11}$$

$$= \left(\mathbf{H_j H_j^H} + \sigma_{\mathbf{n}}^{\mathbf{2}}\mathbf{I}\right)\mathbf{\Sigma_j^{-1}}\hat{\mathbf{y}}_j \tag{12}$$

where

$$\begin{aligned}\mathbf{\Sigma_j} =& \mathbf{H_j H_j^H} + \mathbf{H_{1:j-1}}\overline{\mathbf{\Phi}}^{\mathrm{post}}\mathbf{H_{1:j-1}^H} \\ &+ \mathbf{H_{j+1:J}}\overline{\mathbf{\Phi}}^{\mathrm{pri}}\mathbf{H_{j+1:J}^H} + \sigma_{\mathbf{n}}^{\mathbf{2}}\mathbf{I}\end{aligned} \tag{13}$$

and $\overline{\mathbf{\Phi}}^{\mathrm{post}} = \mathrm{diag}(\overline{\lambda}_1^{\mathrm{post}}, \cdots, \overline{\lambda}_{j-1}^{\mathrm{post}})$ and $\overline{\mathbf{\Phi}}^{\mathrm{pri}} = \mathrm{diag}(\overline{\lambda}_{j+1}^{\mathrm{pri}}, \cdots, \overline{\lambda}_J^{\mathrm{pri}})$ are the covariance matrices for $\mathbf{x_{1:j-1}}$ and $\mathbf{x_{j+1:J}}$, respectively. $\overline{\lambda}_j^{\mathrm{post}}$ is given by [1], [24]

$$\overline{\lambda}_i^{\mathrm{post}} = \sum_{\theta\in\Theta} |\theta - \overline{x}_i^{\mathrm{post}}|^2 \prod_{k=1}^{Q} \underbrace{\frac{1}{2}\left(1 + \overline{c}_{i,k}\tanh\left(L_{\mathrm{post}}(\overline{c}_{i,k})/2\right)\right)}_{Pr(\overline{c}_{i,k})}. \tag{14}$$

$\overline{\lambda}_i^{\mathrm{pri}}$ is defined in the similar way. Note that the reason of diagonal assumption on the covariance matrix $\overline{\mathbf{\Phi}}^{\mathrm{post}}$ and $\overline{\mathbf{\Phi}}^{\mathrm{pri}}$ is because information bits (in a codeblock) are scrambled via the random interleaver so that the symbols in a symbol vector $\mathbf{x}$, generated by information bits, are approximately statistically independent. We show in subsection III-C that this MMSE interference suppression step effectively improves the performance of group detection especially when the *a priori* information on the symbols is absent or weak.

Denoting $\mathbf{W_j} = \left(\mathbf{H_j H_j^H} + \sigma_{\mathbf{n}}^{\mathbf{2}}\mathbf{I}\right)\mathbf{\Sigma_j^{-1}}$, (12) can be rewritten as

$$\hat{\mathbf{z}}_j = \mathbf{W_j}\left(\mathbf{y} - \mathbf{H_{1:j-1}}\overline{\mathbf{x}}^{\mathrm{post}} - \mathbf{H_{j+1:J}}\overline{\mathbf{x}}^{\mathrm{pri}}\right). \tag{15}$$

From (15), we observe that the preprocessing is performed by the cancellation of the inter-group interference followed by the application of the linear clean-up operator $\mathbf{W_j}$.

B.3 SSG Detection

One can simply express (15) as

$$\hat{\mathbf{z}}_j = \mathbf{W_j H_j x_j} + \mathbf{v_j} \tag{16}$$

where $\mathbf{v_j} = \mathbf{W_j}(\mathbf{H_{1:j-1}}(\mathbf{x_{1:j-1}} - \overline{\mathbf{x}}^{\mathrm{post}}) + \mathbf{H_{j+1:J}}(\mathbf{x_{j+1:J}} - \overline{\mathbf{x}}^{\mathrm{pri}}) + \mathbf{n})$. For simplicity, we assume that the residual interference plus noise $\mathbf{v_j}$ is Gaussian (i.e., $\mathbf{v_j} \sim N(\mathbf{0}, \mathbf{V_j})$ where $\mathbf{V_j} = \mathbf{W_j}\left(\mathbf{\Sigma_j} - \mathbf{H_j H_j^H}\right)\mathbf{W_j^H}$). This approximation is justified by the fact that the approximation error gets smaller as the number of iterations increases (i.e., $\overline{\mathbf{x}}^{\mathrm{post}} \to \mathbf{x_{1:j-1}}$ and $\overline{\mathbf{x}}^{\mathrm{pri}} \to \mathbf{x_{j+1:J}}$). Under this assumption, the *a posteriori* LLRs of $\mathbf{x_j}$ based on $\hat{\mathbf{z}}_i$ becomes

$$\begin{aligned}L'_{\mathrm{post}}(\overline{c}_{k,i}) &= \ln\frac{Pr(\overline{c}_{k,i} = +1|\hat{\mathbf{z}}_j)}{Pr(\overline{c}_{k,i} = -1|\hat{\mathbf{z}}_j)} \\ &= \ln\frac{\sum_{\mathbf{x_j}\in\mathbf{X}_{\mathbf{k,i}}^{+1}}\exp\left(\phi\left(\mathbf{x_j}\right)\right)}{\sum_{\mathbf{x_j}\in\mathbf{X}_{\mathbf{k,i}}^{-1}}\exp\left(\phi\left(\mathbf{x_j}\right)\right)}\end{aligned} \tag{17}$$

where

$$\begin{aligned}\phi(\mathbf{x_j}) =& -\left(\hat{\mathbf{z}}_j - \mathbf{W_j H_j x_j}\right)^H \mathbf{V_j^{-1}}\left(\hat{\mathbf{z}}_j - \mathbf{W_j H_j x_j}\right) \\ &+ \sum_{l=1}^{N_j}\sum_{m=1}^{Q}\overline{c}_{l,m}\frac{L_{\mathrm{pri}}(\overline{c}_{l,m})}{2}.\end{aligned} \tag{18}$$

By plugging $\hat{\mathbf{z}}_j = \mathbf{W_j}\hat{\mathbf{y}}_{\mathbf{j}}$ and $\mathbf{V_j} = \mathbf{W_j}\left(\mathbf{\Sigma_j} - \mathbf{H_j H_J^H}\right)\mathbf{W_j^H}$ into $\phi(\mathbf{x_j})$, we further obtain

$$\begin{aligned}\phi(\mathbf{x_j}) =& -\left(\hat{\mathbf{y}}_j - \mathbf{H_j x_j}\right)^H\left(\mathbf{\Sigma_j} - \mathbf{H_j H_j^H}\right)^{-1}\left(\hat{\mathbf{y}}_j - \mathbf{H_j x_j}\right) \\ &+ \sum_{l=1}^{N_j}\sum_{m=1}^{Q}\overline{c}_{l,m}\frac{L_{\mathrm{pri}}(\overline{c}_{l,m})}{2} \\ =& -\frac{1}{\sigma_n^2}\|\underbrace{\mathbf{F_j}\hat{\mathbf{y}}_{\mathbf{j}}}_{\triangleq\mathbf{d_j}} - \underbrace{\mathbf{F_j H_j}}_{\triangleq\mathbf{Z_j}}\mathbf{x_j}\|^{\mathbf{2}} + \sum_{\mathbf{l=1}}^{\mathbf{N_j}}\sum_{\mathbf{m=1}}^{\mathbf{Q}}\overline{\mathbf{c}}_{\mathbf{l,m}}\frac{\mathbf{L}_{\mathrm{pri}}(\overline{\mathbf{c}}_{\mathbf{l,m}})}{2}\end{aligned} \tag{19}$$

where $\mathbf{F_j} = \sigma_{\mathbf{n}}\left(\mathbf{\Sigma_j} - \mathbf{H_j H_j^H}\right)^{-\mathbf{1/2}}$.

Interestingly, one can observe that the *a posteriori* LLR in (2) has the same form as the LLR in (17) with the exception of employing modified received vector $\mathbf{d_j}$ and system matrix $\mathbf{Z_j}$. This enables us to use any kind of $L \times N_i$-size soft MIMO detector without modification. For example, one can use the list tree search algorithm [1]. Alternatively, if the dimension of the

Table 1. Summary of SSG detector.

STEP 1: (Symbol ordering and grouping) Order symbols $\mathbf{x}$ according to post-detection SINR [23].
Partition $\mathbf{x}$ and $\mathbf{H}$ into the J groups $(\mathbf{x_1}, \mathbf{H_1}), \cdots, (\mathbf{x_J}, \mathbf{H_J})$.
STEP 2: (Loop initialization) Initialize $j = 1$.
STEP 3: (Linear preprocessing) Compute $(\mathbf{d_j}, \mathbf{Z_j})$ from $\mathbf{d_j} = \mathbf{F_j}\hat{\mathbf{y}}_\mathbf{j}$ and $\mathbf{Z_j} = \mathbf{F_j}\mathbf{H_j}$.
STEP 4: (Nonlinear joint detection) Apply a tree detector (e.g., LSD or PDA) to the system $(\mathbf{d_j}, \mathbf{Z_j})$ to find the candidate list for $\mathbf{x_j}$. Calculate the *a posteriori* LLRs (and consequently the extrinsic LLRs) using (20).
STEP 5: Output the extrinsic LLRs of $\mathbf{x_j}$.
Let $j \leftarrow j + 1$.
STEP 6: If $j > J$, finish the loop. Otherwise, go back to STEP 3.

group is small (e.g., $N_i = 2$), one can use an exact APP bit detection by evaluating (17) directly. It is also worth mentioning that with $J = N$ and $N_1, \cdots, N_J = 1$, the SSG detector degenerates to the successive linear detector with *a posteriori* LLR based feedback [25].

Recalling that the complexity of the MIMO detector increases exponentially with the search dimension and the search dimension of the subgroup soft MIMO detector is much smaller than that of the full dimensional soft MIMO detector ($N \geq N_i$), one can expect that the complexity of the subgroup soft MIMO detector is much smaller than that of the full dimensional soft MIMO detector. Indeed, the number of computations in the worst case is reduced from $|F|^N$ to $|F|^{N/J}$ (F is the set of all constellation points), resulting in $\left(|F|^{N(J-1)/J}/J\right)$ −fold decrease in computational complexity. For example, if $N = 8, J = 4$, and 16-QAM ($|F| = 16$) is used, the worst case complexity is reduced from $16^8 (\approx 4 \times 10^9)$ to $4 \times 16^2 (\approx 10^3)$.

In short, the SSG detection operation boils down to the following two steps:

1. Linear preprocessing step: Construct $\mathbf{d_j}(= \mathbf{F_j}\hat{\mathbf{y}})$ and $\mathbf{Z_j}(= \mathbf{F_j}\mathbf{H_j})$. Recall that $\hat{\mathbf{y}}$ is obtained from the received signal vector $\mathbf{y}$ using (8).
2. Nonlinear joint detection: Any nonlinear joint detection schemes can be used. As an example, we can apply a tree detection technique to the system with observation $\mathbf{d_j}$ and the system matrix $\mathbf{Z_j}$ to find candidates of $\mathbf{x_j}$ maximizing $\phi(\mathbf{x_j})$. Then, the *a posteriori* LLR is estimated from

$$L'_{\text{post}}(\overline{c}_{k,i}) \approx \max_{\mathbf{x} \in \mathbf{X}^{+1}_{\mathbf{k,i}} \bigcap \mathbf{\Phi}'}{}^{*} \phi(\mathbf{x}) - \max_{\mathbf{x} \in \mathbf{X}^{-1}_{\mathbf{k,i}} \bigcap \mathbf{\Phi}'}{}^{*} \phi(\mathbf{x}) \quad (20)$$

where Φ' is the candidate list found from the tree search. Finally, the extrinsic LLRs can be obtained from $L'_{\text{ext}}(\overline{c}_{k,i}) = L'_{\text{post}}(\overline{c}_{k,i}) - L_{\text{pri}}(\overline{c}_{k,i})$.

The proposed SSG detection algorithm is summarized in Table 1.

C. Effect of Linear Preprocessing

In this subsection, we investigate the SINR of the SSG detector when the linear MMSE preprocessing is performed. Using (16), the SINR after the linear preprocessing step is expressed as

$$\text{SINR}_j = \frac{E\left[\|\mathbf{W_j}\mathbf{H_j}\mathbf{x_j}\|^2\right]}{E\left[\|\mathbf{v_j}\|^2\right]} \quad (21)$$

$$= \frac{\text{trace}\left(\mathbf{W_j}\mathbf{H_j}\mathbf{H_j^H}\mathbf{W_j^H}\right)}{\text{trace}\left(\mathbf{W_j}\left(\mathbf{\Sigma_j} - \mathbf{H_j}\mathbf{H_j^H}\right)\mathbf{W_j^H}\right)}. \quad (22)$$

Note that as the number of iterations increases, detection quality improves and hence the magnitudes of *a posteriori* and *a priori* LLRs for causal and noncausal group symbols get higher. In the best scenario, $L_{\text{pri}}(\overline{c}_{k,i}) = \ln(Pr(\overline{c}_{k,i} = +1)/Pr(\overline{c}_{k,i} = -1)) \to \infty$ if $Pr(\overline{c}_{k,i} = +1) \to 1$ and $L_{\text{pri}}(\overline{c}_{k,i}) \to -\infty$ if $Pr(\overline{c}_{k,i} = +1) \to 0$ (same interpretation holds for magnitude of *a posteriori* LLRs). Thus, $\mathbf{\Sigma_j} \to \mathbf{H_j}\mathbf{H_j^H} + \sigma_\mathbf{n}^\mathbf{2}\mathbf{I}$ and $\mathbf{W_j} \to \mathbf{I}$ and SINR_j in (22) converges to $\text{trace}(\mathbf{H_j}\mathbf{H_j^H})/(\sigma^\mathbf{2}\mathbf{L})$, which is an ideal SINR without inter-group interferences.

In order to demonstrate the benefit of linear preprocessor, we compare the SINR of the proposed scheme in (22) with the SINR without preprocessing. The average SINRs are numerically evaluated over the MIMO channel whose entries are generated from i.i.d. complex Gaussian $CN(0, 1)$. For convenience, we consider the performance of the processing for the first symbol group ($j = 1$) when no iteration is performed. Figs. 2(a) and (b) show the plots of SINR for various group sizes ($N_1 = 2, 4,$ and 6) and MIMO dimensions ($N = L = 4, 8,$ and 16). Since the group detection without the preprocessing cannot handle the inter-group interference, it is no wonder that the SINR of this system is saturated even with the increase in SNR. Whereas, due to the proper control of the inter-group interference, the SINR of the proposed method grows linearly with the SNR.

IV. CODEBOOK-BASED FEEDBACK AND PRECODING

In this section, we discuss the codebook-based feedback and precoding scheme that allows the MIMO systems using the SSG detector to adapt its precoder based on the channel conditions. Our precoding is aimed at improving the spectral efficiency of the SSG detector by employing the codebook maximizing the sum rate. The overall transceiver structure of the proposed SSG detector using the codebook-based precoding is depicted in Fig. 3. Based on the received data, the SSG detector estimates the output SINR for each data stream and chooses the best procoder (i.e., precoding index) that maximizes the output SINR of the SSG detector. The selected precoding index is sent back to the transmitter and the transmitter multiplies the precoding matrix to the data streams before the data transmission. While an accurate estimation of the SINR is crucial to choose a proper precoder maximizing the spectral efficiency, it is in general very hard to find the closed form expression of the SINR of the nonlinear detector. In this section, we propose a simple yet effective

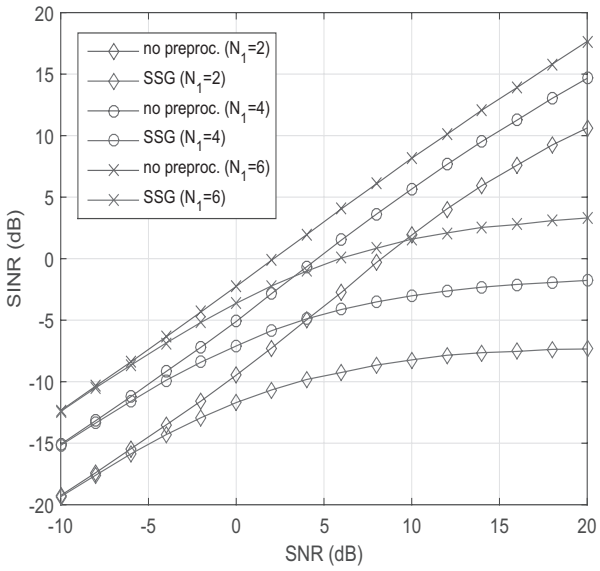

(a)

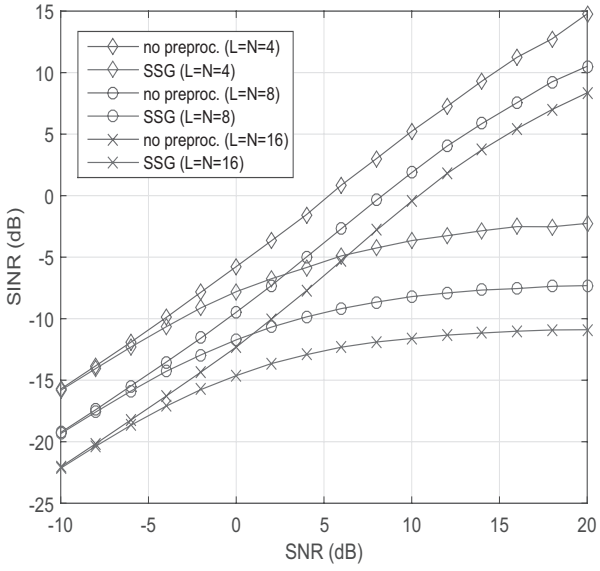

(b)

Fig. 2. Comparison of SINRs between "with preprocessing" and "without preprocessing" cases: (a) $N_1 = 2$ and (b) $N = L = 8$. Performance is measured for the first symbol group when no iteration is performed so that no *a priori* and *a posteriori* information is available in the simulations.

parametric SINR estimation and precoder selection scheme for the SSG detector.

A. Parametric SINR Estimation

When the linear receiver technique such as ZF or MMSE receiver is applied, the closed form expression of the SINR for each multiplexed stream can be obtained easily [26]. Since such is not the case for the nonlinear detection scheme including the SSG detector, we consider an indirect method exploiting the upper and lower bounds of the SINR. The main idea of the proposed approach is that the SINR of the SSG detector is upper

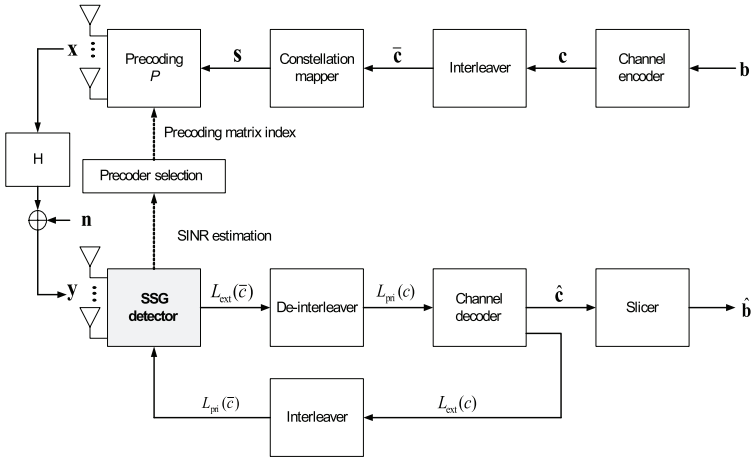

Fig. 3. The overall transceiver diagram of the proposed SSG detector with precoding.

bounded by the SINR with perfect LLRs and lower bounded by the SINR with no LLRs. When the upper and lower bounds of the SINR are found, it is clear that the SINR of the SSG detector lies between these two. Therefore, by a simple matching between the empirical SINR and parameterized SINR, one can obtain a reasonably good SINR estimate of the proposed scheme. Note that the benefit of using a parametric SINR over a measured SINR is that one can predict the SINRs of different precoders without having to send long pilot sequence with different precoders.

We first consider the per-group SINR values of the SSG detector. Let the data rate of the jth group be R_j^{SSG} then

$$R_j^{\text{SSG}} \triangleq \sum_{i=1}^{N_j} R_{j,i}^{\text{SSG}} = \sum_{i=1}^{N_j} \log_2(1+\gamma_{j,i}^{\text{SSG}}) \tag{23}$$

where $\gamma_{j,i}^{\text{SSG}}$ is the SINR of the ith stream at the jth group and N_j is the number of streams for the group j. Then, the sum rate R^{SSG} of the SSG detector becomes

$$R^{\text{SSG}} = \sum_{j=1}^{J} R_j^{SSG} = \sum_{j=1}^{J}\sum_{i=1}^{N_j} \log_2(1+\gamma_{j,i}^{\text{SSG}}). \tag{24}$$

Since per-group SINR values $\{\gamma_{j,i}^{\text{SSG}}\}_{i=1}^{N_j}$ cannot be explicitly obtained, we first compute the upper and lower bounds of $\gamma_{j,i}^{\text{SSG}}$. As a lower bound of $\gamma_{j,i}^{\text{SSG}}$, the SINR of the linear MMSE receiver without LLR feedbacks can be considered. Recall that the output of the linear preprocessing step for the jth group detection in (16) is $\hat{\mathbf{z}}_j = \mathbf{W_j H_j x_j} + \mathbf{v_j}$. When the LLR is unavailable (i.e., all LLR values are zero), the covariance matrix of estimation errors for the jth symbol group is given by [27, Chapter

11]

$$\mathbf{M_j} = \mathrm{Cov}(\mathbf{x_j}, \mathbf{x_j}) - \mathrm{Cov}(\mathbf{x_j}, \hat{\mathbf{z}}_\mathbf{j})\mathrm{Cov}(\hat{\mathbf{z}}_\mathbf{j}, \hat{\mathbf{z}}_\mathbf{j})^{-1}\mathrm{Cov}(\mathbf{x_j}, \hat{\mathbf{z}}_\mathbf{j})^{\mathbf{H}} \tag{25}$$

$$= \mathbf{I}_{\mathbf{N_j}} - \mathbf{H_j^H W_j^H} \left(\mathbf{W_j H_j H_j^H W_j^H} + \mathbf{V_j}\right)^{-1} \mathbf{W_j H_j} \tag{26}$$

$$= \mathbf{I}_{\mathbf{N_j}} - \mathbf{H_j^H W_j^H} \left(\mathbf{W_j} \left(\mathbf{HH^H} + \sigma_\mathbf{n}^\mathbf{2}\mathbf{I}\right) \mathbf{W_j^H}\right)^{-1} \mathbf{W_j H_j} \tag{27}$$

$$= \mathbf{I}_{\mathbf{N_j}} - \mathbf{H_j^H} \left(\mathbf{HH^H} + \sigma_\mathbf{n}^\mathbf{2}\mathbf{I}\right)^{-1} \mathbf{H_j} \tag{28}$$

where we used $\mathbf{V_j} = \mathbf{W_j}\left(\mathbf{\Sigma_j} - \mathbf{H_j H_j^H}\right)\mathbf{W_j^H} = \mathbf{W_j}\left(\mathbf{H_{1:j-1} H_{1:j-1}^H} + \mathbf{H_{j+1:J} H_{j+1:J}^H}\right)\mathbf{W_j^H}$. Using $\mathrm{SINR}_{j,i} = 1/\mathrm{MMSE}_{j,i} - 1$ [28][4], we have

$$\gamma_{j,i}^{\mathrm{mmse}} = \frac{1}{[\mathbf{M}_j]_{i,i}} - 1 \tag{29}$$

and the corresponding sum rate R^{mmse} is given by

$$R^{\mathrm{mmse}} = \sum_{j=1}^{J}\sum_{i=1}^{N_j} R_{j,i}^{\mathrm{mmse}} = \sum_{j=1}^{J}\sum_{i=1}^{N_j} \log_2 \frac{1}{[\mathbf{M}_j]_{i,i}} \tag{30}$$

where $[\mathbf{A}]_{\mathbf{k,l}}$ denotes (k,l)-th entry of a matrix $\mathbf{A}$. It is easy to show that the SINR in (29) is lower than that with nonzero LLR feedback (see Appendix VI).

Next, as an upper bound of $\gamma_{j,i}^{\mathrm{SSG}}$, the SINR of receiver employing interstream interference cancellation (IIC) with perfect LLR feedbacks can be considered. When the inter-group interference is removed perfectly via the linear preprocessor, the output of jth group becomes $\hat{\mathbf{z}}_j = \mathbf{H_j x_j} + \mathbf{n_j} = \sum_\mathbf{i} \mathbf{h_j^i x_{j,i}} + \mathbf{n_j}$, where $\mathbf{h_j^i}$ denotes the ith column vector of $\mathbf{H_j}$. Further, when the intra-group interference is removed perfectly, the upper bound of detection performance can be achieved. In this case, the received SINR of the ith stream at the jth group becomes

$$\gamma_{j,i}^{\mathrm{IIC}} = \frac{1}{\sigma_n^2}\|\mathbf{h_j^i}\|^\mathbf{2}. \tag{31}$$

The corresponding sum rate R^{IIC} becomes

$$R^{\mathrm{IIC}} = \sum_{j=1}^{J}\sum_{i=1}^{N_j} R_{j,i}^{\mathrm{IIC}} = \sum_{j=1}^{J}\sum_{i=1}^{N_j} \log_2\left(1 + \frac{1}{\sigma_n^2}\|\mathbf{h_j^i}\|^\mathbf{2}\right). \tag{32}$$

Using (30) and (32), we have $\gamma_{j,i}^{\mathrm{mmse}} \le \gamma_{j,i}^{SIG} \le \gamma_{j,i}^{\mathrm{IIC}}$, which in turn implies that

$$R^{\mathrm{mmse}} \le R^{\mathrm{SSG}} \le R^{\mathrm{IIC}}. \tag{33}$$

In order to estimate the SINR $\{\gamma_{j,i}^{\mathrm{SSG}}\}_{i=1}^{N_j}$, we first define the ratio $\kappa_{j,i}$ as

$$\kappa_{j,i} = \frac{R_{j,i}^{\mathrm{SSG}} - R_{j,i}^{\mathrm{mmse}}}{R_{j,i}^{\mathrm{IIC}} - R_{j,i}^{\mathrm{mmse}}}, \quad 0 \le \kappa_{j,i} \le 1. \tag{34}$$

[4]$\mathrm{SINR}_{j,i}$ and $\mathrm{MMSE}_{j,i}$ are defined as the SINR and the MMSE for the ith stream of the jth group when the linear MMSE detector is used.

For analytic simplicity, we assume that all streams in a group have the same capacity ratio ($\kappa_j = \kappa_{j,1} = \cdots = \kappa_{j,N_j}$). Then we have

$$\kappa_j = \frac{R_j^{\mathrm{SSG}} - R_j^{\mathrm{mmse}}}{R_j^{\mathrm{IIC}} - R_j^{\mathrm{mmse}}}. \tag{35}$$

Although this assumption is not strictly true, it works well in many practical MIMO systems with spatially rich scattering and fixed modulation order[5]. After some manipulations, for all $1 \le i \le N_j$, we have

$$R_{j,i}^{\mathrm{SSG}} = \kappa_j R_{j,i}^{\mathrm{IIC}} + (1-\kappa_j) R_{j,i}^{\mathrm{mmse}}. \tag{36}$$

Now, by plugging $R_{j,i}^{\mathrm{mmse}} = \log_2\left(1+\gamma_{j,i}^{\mathrm{mmse}}\right)$ and $R_{j,i}^{\mathrm{IIC}} = \log_2\left(1+\gamma_{j,i}^{\mathrm{IIC}}\right)$ into (36), the SINR of the ith stream at the group j for the SSG detector can be expressed as

$$\begin{aligned}\gamma_{j,i}^{\mathrm{SSG}} &= \left(1+\gamma_{j,i}^{\mathrm{IIC}}\right)^{\kappa_j}\left(1+\gamma_{j,i}^{\mathrm{mmse}}\right)^{1-\kappa_j} - 1 \\ &= \left(1 + \frac{1}{\sigma_n^2}\|\mathbf{h_j^i}\|^\mathbf{2}\right)^{\kappa_j}\left([\mathbf{M}_j]_{i,i}\right)^{\kappa_j - 1} - 1 \\ &= \left(1 + \frac{1}{\sigma_n^2}\|\mathbf{h_j^i}\|^\mathbf{2}\right)^{\kappa_j} \\ &\quad \cdot \left(1 - \left(\mathbf{h_j^i}\right)^H \left(\mathbf{HH^H} + \sigma_\mathbf{n}^\mathbf{2}\mathbf{I}\right)^{-1}\mathbf{h_j^i}\right)^{\kappa_j - 1} - 1\end{aligned} \tag{37}$$

Since $\gamma_{j,i}^{\mathrm{IIC}}$ and $\gamma_{j,i}^{\mathrm{mmse}}$ can be computed once the channel matrix $\mathbf{H}$ is available, what remains is to optimize κ_j. In fact, κ_j is chosen to provide the best fitting accuracy between the measured SINR and the parameterized SINR within its range as

$$\hat{\kappa}_j = \underset{0\le\kappa_j\le 1}{\arg\min} \sum_{i=1}^{N_j} \left|\hat{\gamma}_{j,i} - \gamma_{j,i}^{\mathrm{SSG}}\right|^2 \tag{38}$$

where $\hat{\gamma}_{j,i}$ is the measured SINR obtained from the pilot signal.[6]

B. Precoding for High-Dimensional Antenna Systems

In this subsection, we discuss the codebook-based precoding for high-dimensional MIMO systems. Depending on whether a finite number of precoding matrices are used or not, the closed-loop MIMO system can be classified into the codebook and non-codebook-based systems[7]. Since the direct feedback of the CSI incurs too much overhead in the feedback link (uplink)[8], the

[5]Under spatially rich scattering and fixed modulation, all entries of channel matrix has i.i.d. Rayleigh distribution and statistics of all symbols are identical. Hence, all streams in a symbol group go through the same amount of interferences and hence, we can readily assume that the capacity ratios for all streams are the same.

[6]Since the pilot observation $\mathbf{y_p}$ is modeled as $\mathbf{y_p^{[n]}} = \mathbf{hs_p} + \mathbf{v^{[n]}}$ where $\mathbf{s_p}$ is the known pilot signal, under the assumption that the channel $\mathbf{h}$ is stationary, noise power is $\sigma_v^2 = (1/2)\,E|d[n]|^2$ where $d[n] = \mathbf{y_p^{[n]}} - \mathbf{y_p^{[n-1]}}$ is the difference of pilot observations and hence the SINR estimate $\hat{\gamma}$ is $\hat{\gamma} = E|\mathbf{hs}|^\mathbf{2}/E|\mathbf{v}|^\mathbf{2} = \left(E|\mathbf{y}|^\mathbf{2} - \hat{\sigma}_\mathbf{v}^\mathbf{2}\right)/\hat{\sigma}_v^2$.

[7]The closed-loop MIMO means that the transmitter adapts its data transmission strategy in response to the channel feedback sent by the receiver. In the open-loop MIMO, no feedback is sent from the receiver so the transmitter has no knowledge about the channel states.

[8]Since the feedback of real numbered CSI would require an infinite number of bits and hence is impractical, by the quantization process the CSI is expressed as a finite number of bits. Considering the feedback overhead, codebook-based precoding has been adopted in 3GPP LTE and LTE-Advanced standard [29].

codebook-based precoding is a reasonable option for the high-dimensional MIMO systems [30]. Under this mode, mobile receiver estimates the CSI from the pilot signal (e.g., reference signal in 3GPP LTE) sent by the base station and then feeds back an index of the precoding matrix so called precoding matrix indicator (PMI). In the codebook-based precoding scheme, the precoding matrix $\mathbf{P}$ maximizing the spectral efficiency is chosen among multiple candidate matrices. In this paper, we put our focus on the codebook for 8 transmit antennas for the sake of simplicity. However, the extension to more than 8 antenna scenario would be straightforward.

As a simple way to obtain 8 transmit antenna codebook, we integrate 2 transmit antenna and 4 transmit antenna codebooks. The codewords can be obtained from the rotated-DFT reflection $P(m,n) = (1/\sqrt{L})\exp(j\,(2\pi/L)\,m(n+g/G))$ where $g = 0, 1, \cdots, G-1$ and G denotes the number of generated codebooks [31]. In the sequel, we denote the codebook associated with the l transmit antennas as $\mathbf{P^{(l)}}$. For 2 transmit antenna case, $m \in \{0,1\}, n \in \{0,1\}$, and $G = 4$. For 4 transmit antenna case, $m \in \{0,\cdots,3\}, n \in \{0,\cdots,3\}$, and $G = 16$. By combining these two, we obtain the codebook for 8 transmit antenna case as

$$\mathbf{P^{(8)}} = \left(\mathbf{P^{(2)}}\right)^{\mathbf{H}} \otimes \left(\mathbf{P^{(4)}}\right)^{\mathbf{H}} \tag{39}$$

where $\otimes$ denotes the Kronecker product. In addition, in order to have low peak-to-average-power (PAPR), the codebook should satisfy the constant modulus property, which implies that all the matrix elements have equal absolute value [32]. In fact, this property is one of main features of the codebook for 3GPP LTE and LTE-Advanced standard [33]. When b feedback bits are used, we have 2^b precoding matrices in total. Among these, the best precoder $\mathbf{P}^*$ maximizing the spectral efficiency is chosen as

$$\mathbf{P}^* = \arg\max_{\mathbf{P^{(8)}}} \sum_{\mathbf{j=1}}^{\mathbf{J}} \sum_{\mathbf{i=1}}^{\mathbf{N_j}} \log_{\mathbf{2}} \left(\mathbf{1} + \gamma_{\mathbf{j,i}}^{\mathrm{SSG}}(\hat{\kappa}_{\mathbf{j}}, \mathbf{P^{(8)}})\right) \tag{40}$$

where $\gamma_{j,i}^{\mathrm{SSG}}(\hat{\kappa}, \mathbf{P^{(8)}})$ is the estimated SINR when the precoding matrix $\mathbf{P^{(8)}}$ is applied. After choosing $\mathbf{P}^*$, the mobile receiver sends the chosen index (PMI) to the transmitter.

V. SIMULATION RESULTS

In this section, we evaluate the performance of the SSG detector through computer simulations. We first investigate the open-loop performance and complexity of the SSG detector and existing soft-output detectors and then study the link level performance of the SSG detector with the proposed precoding scheme.

A. Simulation Setup

In the simulation setup, we test the soft detection algorithms including the proposed SSG detector. A total of 2×10^5 information bits are randomly generated. A rate R punctured turbo code using the same constituent codes with feedback polynomial $1 + D + D^2$ and feedforward polynomial $1 + D^2$ is employed. We use a random interleaver of size of $12,000$ bits. As a channel model, we use the i.i.d. Rayleigh fading channels where each entry of $\mathbf{H}$ is i.i.d. complex Gaussian $CN(0,1)$. For the channel decoding, two max-log MAP decoders [3] are used to generate the extrinsic LLRs via iterative decoding. Note that the overall system performs two types of iterative decoding operations: 1) The inner-loop decoding performed for IDD iterations and 2) the outer-loop decoding for turbo decoding. Note that for each IDD iteration, a total of eight outer iterations are performed for channel decoding (punctured Turbo decoding). The SNR used for performance evaluation is defined as $\mathrm{SNR} = 10\log_{10}(N_t/\sigma_n^2)$. Note that the signal power used in SNR accounts for the total power from all transmit antennas. Computational complexity of detectors is measured by counting the average number of complex multiplications. The number of IDD iterations is also considered in evaluating detector complexity.

B. Simulation Results

We compare the performance of the proposed SSG detector with the following IDD detection schemes;

- List sphere decoder (LSD) $(|S|, r)$ [1]: $|S|$ denotes the size of candidate list for candidate search and r determines the initial radius of sphere search (i.e., initial radius = $rN\sigma_n^2$). We set $|S| = 1024, r = 2$ as used in the original paper [1].
- K-best algorithm (K) [11]: K best candidates are searched for each layer of the search tree and these candidates are used in the generation of the extrinsic LLRs. The algorithm is parameterized by K. In our simulations, we set $K = 36$.
- MMSE-PIC [2], [21]: The soft-output MMSE-PIC was initially proposed in the context of multi-user detection. With the aid of soft interference estimate, the linear detector performs the parallel interference cancellation.

Note that the post-detection SINR-based symbol ordering [23] is performed before the LSD, K-best detection, and SSG detection. In the LSD and K-best detector, we convert the system matrix into an upper triangular form using the QR decomposition and then conduct tree search in the triangular structured lattice [4]. As a group detector, the SSG detector employs the exact APP bit detection for group size $N_k = 2$ and LSD with $|S| = 512$ and $|S| = 1024$ for group size $N_k = 3$ and 4, respectively. Note also that since the dimension of each group is small, computational complexity associated with these group detectors is moderate.

In Fig. 4, we plot the performance and complexity of the soft-input soft-output detectors for 8×8 MIMO system ($L = N = 8$) with 16-QAM modulation. The code rate R is set to $1/2$. In the SSG detector, all symbols are partitioned into four symbol groups ($J = 4$ and $N_k = 2$, $k = 1, \cdots, 4$). Note that the performance of each algorithm is evaluated after bit error rate (BER) performance converges. As a metric to measure the complexity, we use the number of complex multiplications. Among three benchmark algorithms, LSD achieves the best performance at the expense of large cost in computational complexity. As mentioned, when the dimension of MIMO systems increases, the K-best algorithm exhibits large gap in performance from LSD due to the greedy nature of the algorithm. Whereas, the SSG algorithm yields the performance close to the LSD while achieving substantial reduction in complexity (80% and 65% reduction

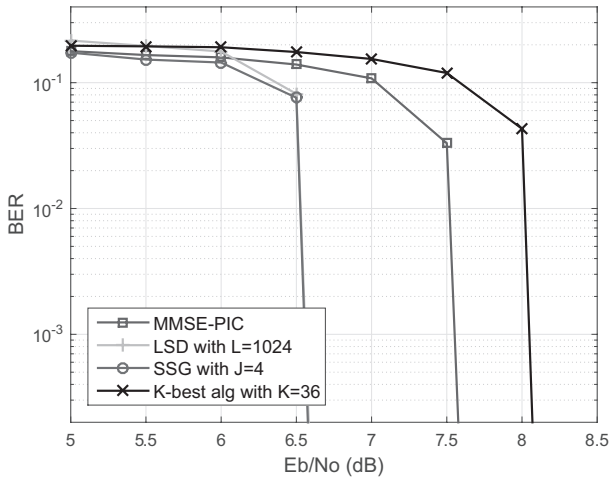

(a)

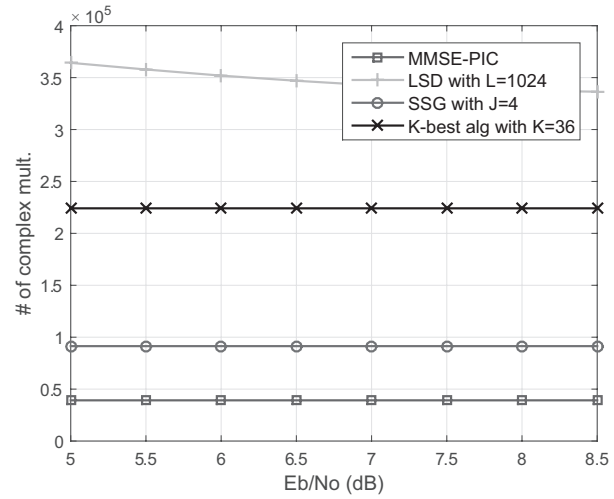

(b)

Fig. 4. Performance and complexity of various IDD detection schemes for 8×8 MIMO systems with 16-QAM modulation (code rate $R = 1/2$): (a) BER performance and (b) complexity.

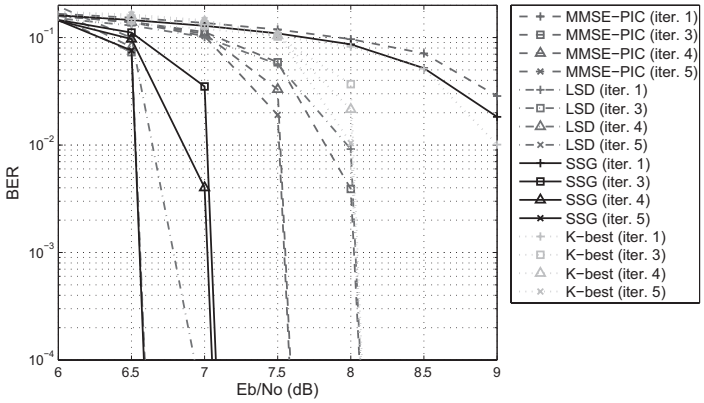

Fig. 5. Performance convergence of various IDD detection schemes for 8×8 MIMO systems with 16-QAM modulation (code rate $R = 1/2$).

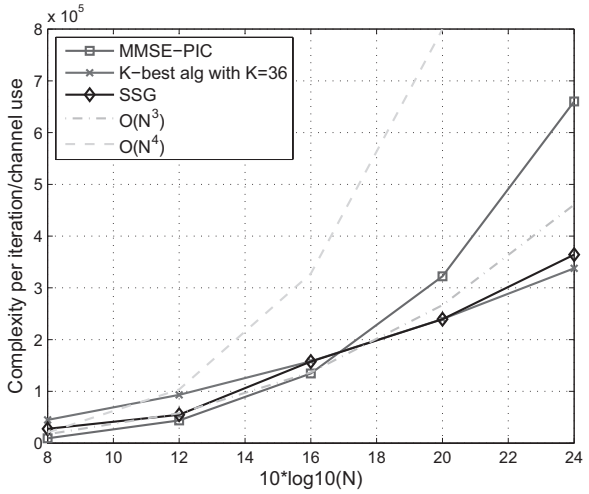

Fig. 6. Computational complexity of various IDD detection schemes as a function of N when 16-QAM modulation is used (code rate $R = 2/3$).

over LSD at 7 dB Eb/No, respectively). Although the computational complexity of the SSG algorithm is slightly higher than that of MMSE-PIC, the SSG algorithm provides more than 1 dB gain over MMSE-PIC.

In Fig. 5, we plot the performance of the IDD detectors for various number of iterations. The simulation setup is the same as that used in Fig. 4. We observe that the performance of MMSE-PIC, K-best, and SSG detectors converges within five iterations while that of LSD converges within three iterations. Although the number of iterations of LSD is less than the rest of detectors, the computational overhead is still overwhelming.

We next investigate how performance and complexity of the soft-output detectors behave when the system dimension increases. Toward this end, we evaluate the performance of IDD detectors for $N(= L) = 8,\ 12,\ 16,\ 20$, and 24. For each of N value, the SSG parameter J is set to $3,\ 3,\ 4,\ 5$, and 6, respectively. Denoting the size of the ith symbol group by N_i, the grouping is done with $(N_1, N_2, N_3, N_4) = (3, 3, 2, 0), (3, 3, 3, 3), (4, 4, 4, 4), (5, 5, 5, 5)$, and $(6, 6, 6, 6)$. In our simulations, the code rate is set to $R = 2/3$ and 16-QAM modulation is used. We note that we could not add the result of LSD due to its tremendous complexity for large N. Computational complexity of the detectors as a function of N is shown in Fig. 6 and the performance gain of the SSG detector over the MMSE-PIC detector and the K-best detector is summarized in Table 2. Though the complexity of the SSG detector is slightly higher than that of the MMSE-PIC for $N = 8$ to 16 (the complexity is even better for $N = 20$ and 24), the SSG detector achieves around 1.5 dB performance gain over the MMSE-PIC for all N values considered. Due to the use of small group size, when $N \geq 20$, the computational overhead of the SSG detector becomes even smaller than that of MMSE-PIC. While there is no performance gap between the K-best algorithm and the SSG detector for $N = 8$ and 12, the gap gradually increases with N. To achieve the comparable performance to the SSG detector, the candidate size K should be increased, which will cause large computational cost. In our setup, we observe that the SSG detector achieves up to 35% reduction in complexity over the K-best algorithm. Note that the complexity of the SSG detector

Table 2. Performance of the SSG detector vs. N when 16-QAM modulation is used (code rate $R = 2/3$).

N	8	12	16	20	24
Performance gain over MMSE-PIC	1.5 dB	1.5 dB	1.5 dB	1.5 dB	1.5 dB
Performance gain over K-best algorithm ($K = 36$)	0 dB	0 dB	0.5 dB	1.5 dB	2.0 dB

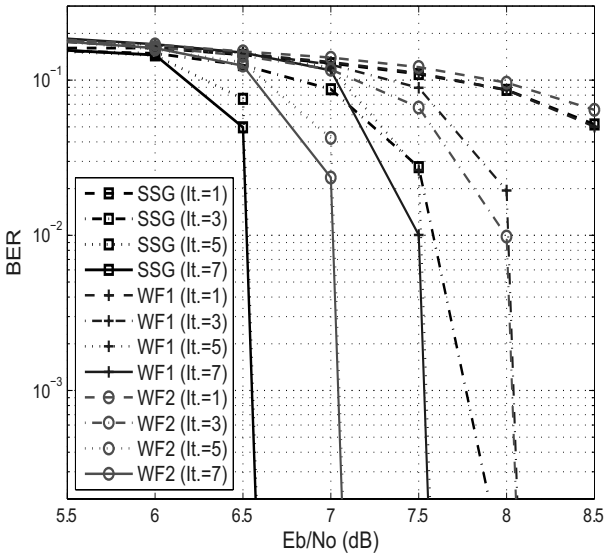

Fig. 7. BER performance of the IDD group detectors with different preprocessing strategies for 8×8 MIMO systems with 16-QAM modulation (code rate $R = 1/2$).

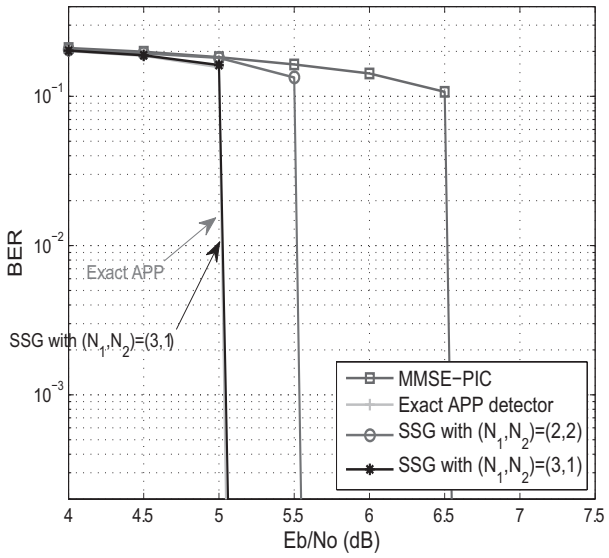

Fig. 8. Performance of the IDD detectors and the optimal APP bit detector for 4×4 MIMO systems with 16-QAM modulation (code rate $R = 1/2$).

increases with N at moderate pace. When N becomes so large, we can further control the complexity by using a small group size (e.g., $J = 2$ or 3). We also observe from Fig. 4 and Table 2 that the performance gain of the SSG detector over the K-best algorithm is higher when a lower code rate R is used, which demonstrates that the proposed preprocessing scheme exploits the LLRs from the channel decoder effectively.

Next, we observe the performance of the SSG detector with different preprocessing algorithms used in [16] and [17]. For fair comparison, the same number of groups ($J = 4$) is employed and the code rate $R = 1/2$ is used. For convenience, we denote the preprocessing methods of [16] and [17] as whitening preprocessing filter (WF) 1 and 2, respectively. WF1 and WF2 whiten the noise plus interfering symbol groups before the group detection, which requires $L \times L$ matrix inversion for the coefficient calculation and $L \times 1$ multiplication for the linear filtering. Hence, the complexity of WF1 and WF2 is more or less similar to that of the SSG detector. Fig. 7 shows the BER performance of three preprocessing algorithms for various number of iterations. In general, we observe that the gain of the SSG detector over whitening filters improves as the number of iterations increases, which demonstrates that the proposed MMSE preprocessor is effective in suppressing the inter-group interference.

It might be of interest to compare the performance of the SSG detector with the optimal APP bit detector. Since the complexity of the APP bit detector increases dramatically with the system size, we only consider 4×4 systems with 16-QAM modulation. Fig. 8 shows the BER performance of the SSG, MMSE-PIC, and optimal APP bit detectors. Two distinct grouping configurations ($(N_1, N_2) = (2, 2), (3, 1)$) are considered for the SSG detector. Note that the SSG detector with $(N_1, N_2) = (3, 1)$ performs almost identical to the exact APP bit detector and outperforms the MMSE-PIC detector. When the configuration is changed to $(N_1, N_2) = (2, 2)$, the SSG detector exhibits a slight gap (around 0.5 dB loss) in performance from the exact APP bit detector.

In order to observe comprehensive picture on link level performance, we plot the average throughput of the closed-loop and open-loop systems in Fig. 9. In this setup, the system supports 8 streams (with code rate $R = 1/2$) and 16-QAM modulation is used so that the maximum throughput per channel realization becomes 16 (bps/Hz). In our simulations, we compute the average throughput by counting the number of correctly decoded bits. As a precoder, we use 8 transmit antenna codebook in (39) and the feedback bits of the codebook are set to 6. The SINR of the SSG detector is estimated from the steps described in (37) and (38) in subsection IV-A and that of the MMSE-PIC detector is obtained in a closed form [21]. As shown in Fig. 9, MMSE-PIC achieves the maximal throughput at 7.5 dB and the proposed SSG detector achieves the maximal throughput at 6.6 dB, offering around 1 dB gain in the system throughput.

Finally, we investigate the performance of the IDD system for correlated channels in larger MIMO systems ($L = N = 16$). We set the size of each symbol group to $J = 2$. The correlation

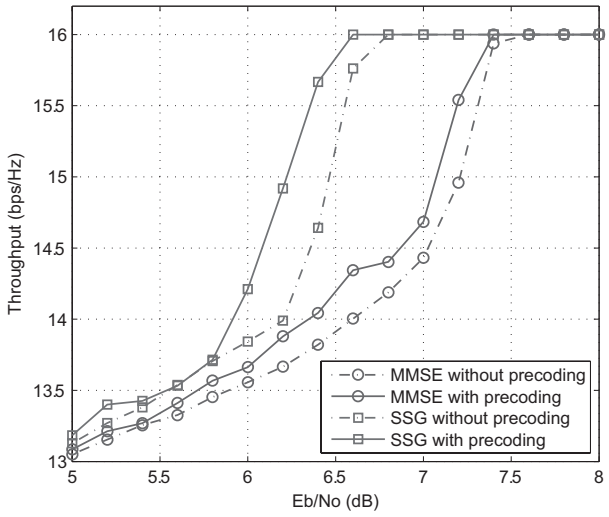

Fig. 9. Average throughput of the SSG detector and MMSE-PIC receiver for 8×8 MIMO systems with 16-QAM modulation (code rate $R = 1/2$).

coefficients between the adjacent transmit antennas are set to $\alpha = 0$ and $\alpha = 0.1$ in Figs. 10 (a) and 10 (b), respectively. Such correlated channel is generated by $\mathbf{HR^{1/2}}$, where $\mathbf{H}$ is the i.i.d. channel matrix and $\mathbf{R}$ is the transmit antenna correlation matrix given by

$$\mathbf{R} = \begin{bmatrix} 1 & \alpha & \cdots & \alpha^N \\ \alpha & 1 & \cdots & \alpha^{N-1} \\ \vdots & \vdots & \ddots & \vdots \\ \alpha^N & \alpha^{N-1} & \cdots & 1 \end{bmatrix}. \tag{41}$$

In this test, we do not consider the LSD detector and focus only on the SSG detector and the MMSE-PIC due to the computational burden. When there is no antenna correlations, i.i.d. channel matrix $\mathbf{H}$ is favorable to the MMSE-PIC detector (i.e., $\mathbf{H}^H\mathbf{H} \rightarrow \mathbf{I}$) so that the performance gap between two is small (around 0.5 dB). Whereas, in the presence of the antenna correlation ($\alpha = 0.1$), the performance gain of the SSG detector over the MMSE-PIC increases up to 1 dB. Although we skip further results due to page limitation, we could observe that the performance gap between two detectors increases with antenna correlation.

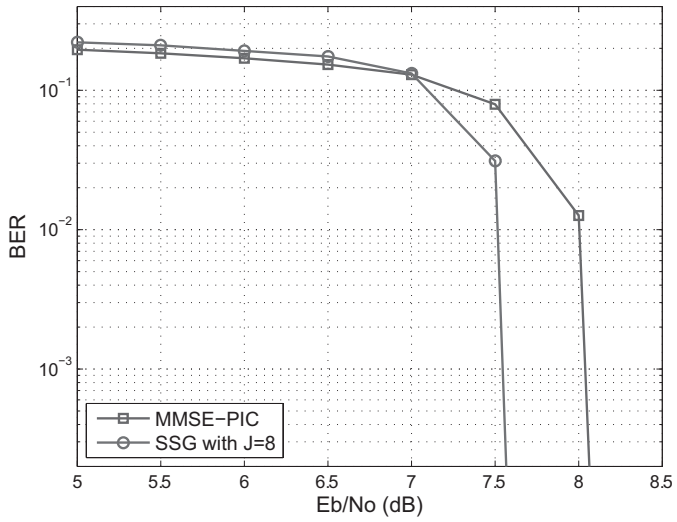

(a)

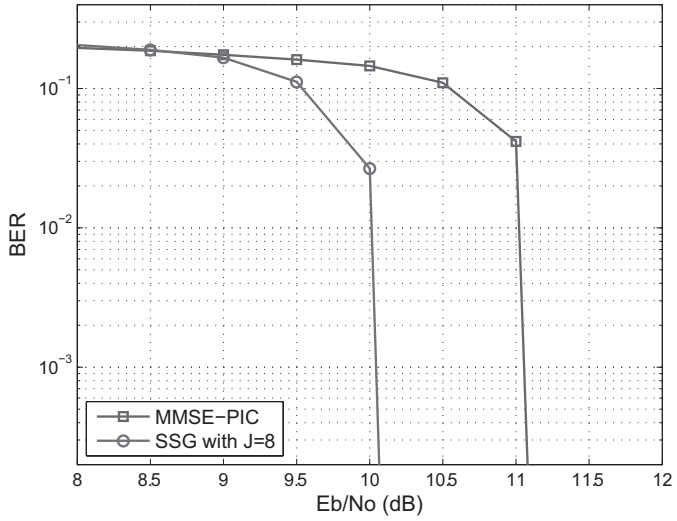

(b)

Fig. 10. BER performance of the SSG detector for 16×16 system with 16-QAM modulation (code rate $R = 1/2$) with (a) no transmit antenna correlation ($\alpha = 0$) and (b) transmit antenna correlation ($\alpha = 0.1$).

VI. CONCLUSIONS

In this paper, we investigated a novel soft-output detection algorithm referred to as the SSG detector, which provides great promise in MIMO systems employing the IDD technique. The proposed SSG detector partitions the symbol vector to be detected into multiple subgroups and then processes each subgroup sequentially. By employing the deliberately designed preprocessing to suppress inter-group interference, the SSG detector can perform the symbol detection in an improved SINR condition and thus achieves performance close to the full dimensional LSD-based soft detector. Further, by adopting a codebook-based precoding for the SSG detector, we could achieve further improvement in the spectral efficiency of the link. Given the importance of the MIMO operation to meet the increasing throughput demands of next generation wireless systems, we believe that the SSG detection algorithm will be a competitive option for the high dimensional MIMO systems. For the successful implementation of this, further studies on implementation issues such as optimal group partitioning, massive codebook design, and fast IDD termination are required. Also, application of the SSG detection into the single carrier systems with frequency-selective channel would be interesting direction to be pursued.

APPENDIX I
PROOF THAT SINR IN (29) IS SMALLER THAN THAT WITH NONZERO LLR FEEDBACK

From (28), the MSE without LLR feedback for the ith symbol in jth group is given by

$$[\mathbf{M}_\mathbf{j}^{(\mathbf{nf})}]_{\mathbf{i},\mathbf{i}} = \mathbf{1} - (\mathbf{h}_\mathbf{j}^\mathbf{i})^\mathbf{H} \underbrace{\left(\mathbf{H}\mathbf{H}^\mathbf{H} + \sigma_\mathbf{n}^\mathbf{2}\mathbf{I}\right)^{-1}}_{\triangleq \mathbf{A}^{-1}} \mathbf{h}_\mathbf{j}^\mathbf{i}$$

where $\mathbf{h}_\mathbf{j}^\mathbf{i}$ is the i-th column vector of the channel matrix for the jth group, $\mathbf{H_j}$. On the other hand, the MSE with LLR feedback is given by

$$[\mathbf{M_j}]_{\mathbf{i},\mathbf{i}} = \mathbf{1} - (\mathbf{h}_\mathbf{j}^\mathbf{i})^\mathbf{H}\mathbf{B}^{-1}\mathbf{h}_\mathbf{j}^\mathbf{i}$$

where

$$\begin{aligned}\mathbf{B} =& \mathbf{H_j}\mathbf{H_j^H} + \mathbf{H_{1:j-1}}\overline{\mathbf{\Phi}}^{\mathrm{post}}\mathbf{H_{1:j-1}^H} \\ &+ \mathbf{H_{j+1:J}}\overline{\mathbf{\Phi}}^{\mathrm{pri}}\mathbf{H_{j+1:J}^H} + \sigma_\mathbf{n}^\mathbf{2}\mathbf{I}.\end{aligned}$$

The difference in MSE becomes

$$[\mathbf{M}_\mathbf{j}^{(\mathbf{nf})}]_{\mathbf{i},\mathbf{i}} - [\mathbf{M_j}]_{\mathbf{i},\mathbf{i}} = (\mathbf{h}_\mathbf{j}^\mathbf{i})^\mathbf{H}\left(\mathbf{B}^{-1} - \mathbf{A}^{-1}\right)\mathbf{h}_\mathbf{j}^\mathbf{i}.$$

Note that $\mathbf{A}-\mathbf{B}$ $(= \mathbf{H_{1:j-1}}\overline{\mathbf{\Phi}}^{\mathrm{post}}\mathbf{H_{1:j-1}^H}+\mathbf{H_{j+1:J}}\overline{\mathbf{\Phi}}^{\mathrm{pri}}\mathbf{H_{j+1:J}^H})$ is positive definite if there is nonzero LLR feedback. Hence, $(\mathbf{B}^{-1} - \mathbf{A}^{-1})$ is also positive definite [34, Corollary 7.7.4], which in turn implies that $[\mathbf{M}_\mathbf{j}^{(\mathbf{nf})}]_{\mathbf{i},\mathbf{i}} > [\mathbf{M_j}]_{\mathbf{i},\mathbf{i}}$. From the relationship between SINR and MMSE, i.e., $\mathrm{SINR}_{i,j} = 1/\mathrm{MMSE}_{i,j} - 1$ [28], we can deduct from $[\mathbf{M}_\mathbf{j}^{(\mathbf{nf})}]_{\mathbf{i},\mathbf{i}} > [\mathbf{M_j}]_{\mathbf{i},\mathbf{i}}$ that SINR without LLR feedback is lower than that with nonzero LLR feedback.

REFERENCES

[1] B. Hochwald and S. T. Brink, "Achieving near-capacity on a multiple-antenna channel," *IEEE Trans. Commun.*, vol. 51, no.3, pp. 389–399, Mar. 2003.

[2] X. Wang and H. V. Poor, "Iterative (Turbo) soft interference cancellation and decoding for coded CDMA," *IEEE Trans. Commun.*, vol. 47, No. 7, pp. 1046–1061, July 1999,

[3] P. Robertson, P. Hoeher, and E. Villebrun, "Optimal and sub-optimal maximum a posteriori algorithms suitable for turbo decoding," *European Trans. on Telecommun.*, vol. 8, no.2, pp. 119–125, Mar. 1997.

[4] A. D. Murugan, H. E. Gamal, M. O. Damen, and G. Caire, "A unified framework for tree search decoding: Rediscovering the sequential decoder," *IEEE Trans. Inform. Theory*, vol. 52, pp. 933–953, Mar. 2006.

[5] U. Fincke and M. Pohst, "Improved methods for calculating vectors of short length in a lattice, including a complexity analysis," *Math. Comput.*, vol. 44, pp. 463–471, Apr. 1985.

[6] J. Choi, B. Shim, and A. Singer, "Efficient soft-input soft-output tree detection via an improved path metric," *IEEE Trans. Inf. Theory*, vol. 58, pp. 1518–1533, Mar. 2012.

[7] J. Lee, B. Shim, and I. Kang, "Soft-input soft-output list sphere detection with a probabilistic radius tightening," *IEEE Trans. Wireless Commun.*, vol. 11, pp. 2848–2857, Aug. 2012.

[8] J. Koo, S. Kim, and J. Kim, "A parallel collaborative sphere decoder for a MIMO communication system," *J. Commun. Netw.*, vol. 16, no. 6, pp. 620–626, Dec. 2014.

[9] L. G. Barbero and T. S. Thompson, "Extending a fixed-complexity sphere decoder to obtain likelihood information for turbo-MIMO systems," *IEEE Trans. Veh. Technol.*, vol. 57, no. 5, pp. 2804–2814, Sept. 2008.

[10] D. W. Water and J. R. Barry, "The chase family of detection algorithms for multiple-input multiple-output channels," *IEEE Trans. Signal Process.*, vol. 56, pp. 739–747, Feb. 2008.

[11] Z. Guo and P. Nilsson, "Algorithm and implementation of the K-best sphere decoding for MIMO detection," *IEEE J. Sel. Areas Commun.*, vol. 24, no. 3, pp. 491–503, Mar. 2006.

[12] J. Hagenauer, and C. Kuhn, "The list-sequential (LISS) algorithm and its application," *IEEE Trans. Commun.* vol. 55, pp. 918–928, May 2007.

[13] M. K. Varanasi, "Group detection for synchronous Gaussian code-division multiple-access channels," *IEEE Trans. Inf. Theory*, vol. 41, no. 4, pp. 1083–1096, July 1995.

[14] J. Luo, K. Pattipati, P. Willett, and G. Levchuk, "Optimal grouping algorithm for a group decision feedback detector in synchronous CDMA communications," *IEEE Trans. Commun.*, vol. 51, no. 3, pp. 341–346, Mar. 2003.

[15] X. Li, H. C. Huang, A. Lozano, and G. J. Foschini, "Reduced-complexity detection algorithms for systems using multi-element arrays," in *Proc. IEEE GLOBECOM*, Dec. 2000, pp. 1072–1076.

[16] A. Elkhazin, K. Plataniotis, and S. Pasupathy, "Reduced-dimension MAP turbo-BLAST detection," *IEEE Trans. Commun.*, vol. 54, no. 1, pp. 108–118, Jan. 2006.

[17] B. Zarikoff, J. K. Cavers, and S. Bavarian, "An iterative groupwise multiuser detector for overloaded MIMO applications," *IEEE Trans. Wireless Commun.*, vol. 6, no. 2, pp. 443–447, Feb. 2007.

[18] J. Choi, B. Shim, A. Singer, and N. Cho, "A low-complexity decoding via reduced dimension maximum likelihood search," *IEEE Trans. Signal Process.*, vol. 58, no. 3, pp. 1780–1793, Mar. 2010.

[19] G. E. Bottomley and Y.-P. E. Wang, "A novel multistage group detection technique and application," *IEEE Trans. Wireless Commun.*, vol. 9, no. 8, pp. 2438–2443, Aug. 2010.

[20] M. Krause, D. P. Taylor, and P. A. Martin, "List-based group-wise symbol detection for multiple signal communication," *IEEE Trans. Wireless Commun.*, vol. 10, no. 5, pp. 1636–1644, May 2011.

[21] M. Sellathurai and S. Haykin, "Turbo-BLAST for wireless communications: theory and experiments," *IEEE Trans. Signal Process.*, vol. 50, pp. 2538–2546, Oct. 2002.

[22] P. W. C. Chan, H. Mow, R. D. Murch, and K. B. Letaief, "The evolution path of 4G networks: FDD or TDD?," *IEEE Commun. Mag.*, vol. 44, no. 12, pp. 42–50, Dec. 2006.

[23] P. W. Wolniansky, G. J. Foschini, G. D. Golden, and R. A. Valenzuela, "V-BLAST: An architecture for realizaing very high data rates over the rich-scattering wireless channel," in *Proc. URSI International Symposium on Signals, Systems, and Electronics*, Sept. 1998, pp. 295–300.

[24] J. Hagenauer, E. Offer, and L. Papke, "Iterative decoding of binary block and convolutional codes," *IEEE Trans. Inf. Theory*, vol. 42, no.2, pp. 429–445, Mar. 1996.

[25] J. Choi, A. C. Singer, J. Lee, and N. I. Cho, "Improved linear soft-input soft-output detection via soft feedback successive interference cancellation," *IEEE Trans. Commun.*, vol. 58, no. 3, pp. 986–996, Mar. 2010.

[26] R. W. Heath, S. Sandhu, and A. J. Paulraj, "Antenna selection for spatial multiplexing systems with linear receivers," *IEEE Commun. Lett.*, vol. 5, no. 4, pp. 142–144, Apr. 2001.

[27] S. M. Kay, *Fundamentals of Statistical Signal Processing: Estimation Theory,* Prentice Hall, 1998.

[28] S. Verdu, *Multiuser Detection*, Cambridge University Press, 2003.

[29] C. Lim, T. Yoo, B. Clerckx, B. Lee, and B. Shim, "Recent trend of multiuser MIMO technologies in LTE-Advanced," *IEEE Comm. Mag.*, pp. 127–135, Mar. 2013.

[30] J. Wang, M. Wu, and F. Zheng, "The codebook design for MIMO precoding systems in LTE and LTE-A," in *Proc. IEEE WiCOM*, Sept. 2010, pp. 1–4.

[31] S. Jia, S. Shiqiang, and Q. Haiyang, *3GPP Long Term Evolution: Principle and System Design*, Posts and Telecom Press, 2008.

[32] B. Clerckx, Y. Zhou, and S. Kim, "Practical codebook design for limited feedback spatial multiplexing," in *Proc. IEEE ICC*, May 2008, pp. 3982–3987.

[33] 3GPP TS 36.213: "Evolved Universal Terrestrial Radio Access (E-UTRA); Physical layer precedures," V9.3.0, Sept. 2010.

[34] R. A. Horn and C. R. Johnson, *Matrix Analysis,* Cambridge, 1985.

Jun Won Choi received the B.S. and M.S. degrees in Electrical and Computer Engineering, Seoul National University and earned Ph.D. degree in Electrical and Computer Engineering, University of Illinois at Urbana-Champaign, respectively. In 2010, he joined Qualcomm, San Diego USA and participated in wireless communication system/algorithm design for commercializing LTE and LTE-A modem chipsets. Since 2013, he has been a Faculty Member of the Department of Electrical Engineering, Hanyang University and is leading Signal Processing and Optimization Research Group. His research area includes wireless communications, signal processing, optimization, data analytic, and machine learning.

Byungju Lee received the B.S. and Ph.D. degrees in the School of Information and Communication, Korea University, Seoul, Korea in 2008 and 2014, respectively. He was a Visiting Scholar with Purdue University, West Lafayette, IN, USA, in 2013. He is presently a Postdoctoral Fellow at Seoul National University. His research interests include information theory and signal processing for wireless communications.

Byonghyo Shim received the B.S. and M.S. degrees in Control and Instrumentation Engineering from Seoul National University, Korea in 1995 and 1997, respectively. He received the M.S. degree in Mathematics and the Ph.D. degree in Electrical and Computer Engineering from the University of Illinois at Urbana-Champaign (UIUC), USA in 2004 and 2005, respectively. From 1997 and 2000, he was with the Department of Electronics Engineering, Korean Air Force Academy as an Officer (First Lieutenant) and an Academic Full-time Instructor. From 2005 to 2007, he was with Qualcomm Inc., San Diego, CA, USA, as a Staff Engineer. From 2007 to 2014, he was with the School of Information and Communication, Korea University, Seoul, as an Associate Professor. Since Sept. 2014, he has been with the Department of Electrical and Computer Engineering, Seoul National University, where he is presently an Associate Professor. His research interests include wireless communications, statistical signal processing, estimation and detection, compressive sensing, and information theory.

Dr. Shim was the recipient of the 2005 M. E. Van Valkenburg Research Award from the Electrical and Computer Engineering Department of the University of Illinois and 2010 Hadong Young Engineer Award from IEIE. He is currently an Associate Editor of the IEEE Wireless Communications Letters, Journal of Communications and Networks, and a Guest Editor of the IEEE Journal on Selected Areas in Communications (JSAC).